ARTICLE
Journal of Cellular Biochemistry 113:3165–3177 (2012)

Journal of Cellular Biochemistry

E2F1-Dependent Pathways are Involved in Amonafide Analogue 7-d-Induced DNA Damage, G2/M Arrest, and Apoptosis in p53-Deficient K562 Cells

Yiquan Li, Jin Shao, Ke Shen, Yufang Xu, Jianwen Liu,* and Xuhong Qian*

State Key Laboratory of Bioreactor Engineering & Shanghai Key Laboratory of Chemical Biology, School of Pharmacy, East China University of Science and Technology, #268, 130 Meilong Road, Shanghai 200237, PR China

ABSTRACT

The E2F1 gene well known is its pivotal role in regulating the entry from G1 to S phase, while the salvage antitumoral pathway which implicates it, especially in the absence of p53, is not fully characterized. We therefore attempted to identify the up- and down-stream events involved in the activation of the E2F1-dependent pro-apoptotic pathway. For this purpose, a amonafide analogue, 7-d (2-(3-(2-(Dimethylamino)ethylamino)propyl)-6-(dodecylamino)-1*H*-benzo[*de*]isoquinoline-1,3(2*H*)-dione) was screened, which exhibited high anti-tumor activity against p53-deficient human Chronic Myelogenous Leukemia (CML) K562 cells. Analysis of flow cytometry and western blots of K562 cells treated with 7-d revealed an appreciable G2/M cycle arrest and apoptosis in a dose and time-dependent manner via p53-independent pathway. A striking increase in "Comet tail" formation and γ-H2AX expression showed that DNA double strand breaks (DSB) were caused by 7-d treatment. ATM/ATR signaling was reported to connect E2F1 induction with apoptosis in response to DNA damage. Indeed, 7-d-induced G2/M arrest and apoptosis were antagonized by ATM/ATR signaling inhibitor, Caffeine, which suggested that ATM/ATR signaling was activated by 7-d treatment. Furthermore, the increased expression of E2F1, p73, and Apaf-1 and p73 dissociation from HDM2 was induced by 7-d treatment, however, knockout of E2F1 expression reversed p73, Apaf-1, and $p21^{Cip1/WAF1}$ expression, reactivated cell cycle progression, and inhibited 7-d-induced apoptosis. Altogether our results for the first time indicate that 7-d mediates its growth inhibitory effects on CML p53-deficient cells via the activation of an E2F1-dependent mitochondrial and cell cycle checkpoint signaling pathway which subsequently targets p73, Apaf-1, and $p21^{Cip1/WAF1}$. J. Cell. Biochem. 113: 3165–3177, 2012.

KEY WORDS: 7-D; K562; G2/M ARREST; APOPTOSIS; DNA DAMAGE; E2F1

Cancer has been one of the most deadly diseases, which has overtaken the heart disease in some developed countries [Rawat, 2008]. Nowadays, the development of new, selective, efficient, and safe drugs for cancer chemotherapy remains an urgent and high priority for medical research needs [Lv and Xu, 2009]. Naphthalimide analogs have been considered as a promising group of anticancer agents by intercalating deoxyribonucleic acid, some of them, e.g., amonafide and mitonafide have reached the clinical trial stage for the treatment of solid tumors and exhibited excellent antitumor activity. However, most clinical trials have failed because of toxic side-effects. Subsequent efforts to improve therapeutic properties of naphthalimides have been made by modifying the naphthalimide skeleton [Gao et al., 2009; Ingrassia et al., 2009].

In the course of screening a series of naphthalimide based DNA intercalators, 7-d (2-(3-(2-(Dimethylamino)ethylamino)propyl)-6-(dodecylamino)-1*H*-benzo[*de*]isoquinoline-1,3(2*H*)-dione) that significantly caused Top-II inhibition and suppressed the growth of multiple cancer cell lines in this series [Chen et al., 2010]. Unlike amonafide, the naphthalimide skeletons of 7-d are fused through to polyamines and long alkyl chains at 2- and 6-positions (Fig. 1). The

Yiquan Li and Jin Shao contributed equally to this work as co-first authors.

Additional supporting material may be found in the online version of this article.

Grant sponsor: Nanotechnology Special Project for Shanghai Committee of Science and Technology; Grant number: 1052nm05400; Grant sponsor: Basic research project of Shanghai Committee of Science and Technology; Grant number: 10JC1414500.

*Correspondence to: Jianwen Liu, or Xuhong Qian, State Key Laboratory of Bioreactor Engineering & Shanghai Key Laboratory of Chemical Biology, School of pharmacy, East China University of Science and Technology, #268, 130 Meilong Road, Shanghai 200237, PR China. E-mail: liujian@ecust.edu.cn; xhqian@ecust.edu

Manuscript Received: 23 September 2011; Manuscript Accepted: 8 May 2012

Accepted manuscript online in Wiley Online Library (wileyonlinelibrary.com): 16 May 2012

DOI 10.1002/jcb.24194 • © 2012 Wiley Periodicals, Inc.

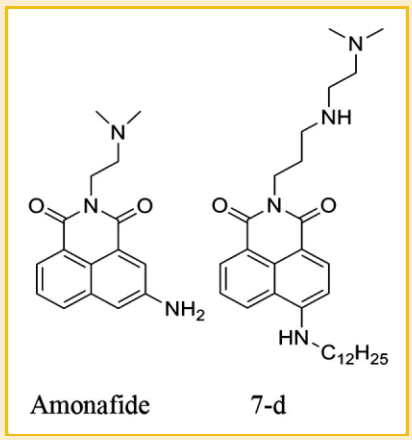

Fig. 1. Chemical structure of Amonafide and 7-d.

addition of polyamines would harness the polyamine transporter (PAT) for drug delivery, which was beneficial for the tumor cell selectivity [Wallace and Palmer, 2010]. Meanwhile, the elimination of the amino group at the 5-position would avoid the amino acetylation that caused unpredictable toxicity of amonafide [Huang et al., 2008].

The growth suppressor p53 plays an important role in preventing cancer development, especially in modulating cell cycle arrest and apoptosis response induced by DNA damage. Though, loss of p53 function occurs in an estimated 50% of all cancers by mutations and deletions including most leukemia cell lines [Blagosklonny, 2002; Di Cintio et al., 2010]. P53 alteration has also been held responsible for the failure of most cancers to respond to chemotherapy [Weller, 1998]. Chronic myelogenous leukemia (CML) cancers are no exception; p53 inactivation plays an important role in the progression of CML to blast crisis [Feinstein et al., 1991]. CML blast crisis (CMLBC) remains a therapeutic challenge because it is highly refractory to standard induction chemotherapy with a response rate in myeloid blast crisis of less than 30% [Karbasian Esfahani et al., 2006]. The typical human K562 leukemic cell line was derived from a patient with CML in acute myeloid blast crisis is relatively resistant to apoptosis induced by a wide range of anticancer agents [Raghuvar Gopal et al., 2005]. Early researches show the p53 gene in the K562 human CML cell line is characterized by a mutation in exon 5, leading to inactivation of this gene [Law et al., 1993].

E2F1, a transcription factor of E2F family, exhibits kinetics that closely resemble the induction of p53 in DNA damage response [Blattner et al., 1999]. Recent researches reported that in the absence of p53, E2F-1 could trigger cell death in responding DNA damage mainly via p73 and Apaf-1 signal pathways. Some researchers even proposed that the E2F1-p73 pathway functions as a backup when p53 is defective to ensure that damaged cells could undergo apoptosis, because in many human tumors that sustain an inactivating mutation of p53, the E2F1-p73 pathway is still intact [Ginsberg and Polager, 2009; Wu and Yu, 2009].

An earlier research had reported the vital role of p53 in naphthalimides analogue induced cell cycle arrest and apoptosis in p53-wt cancer cells [Liang et al., 2011]. However, little attention has been paid to reveal the underlying mechanism of the anticancer effect of naphthalimides analogue in p53-deficient cancer cells. When investigating the chemopreventive potential of 7-d. it showed high antitumor activity against p53-deficient K562 cells in our current study suggesting that the action of 7-d is not affected by p53 status. The mechanism of 7-d action that does not require functional p53 may provide additional treatment options in p53-mutant or deletions CMLBC patients who have shorter survival. Further mechanism researches found that 7-d-induced DNA damage, G2/M arrest and apoptosis in K562 cells accompanied by the activation of E2F1-dependent pathways.

MATERIALS AND METHODS

MATERIALS

7-d and amonafide (>99% pure) were synthesized and provided as described previously [Chen et al., 2010]. A 20 mM stock solution of 7-d was prepared with dimethyl sulfoxide (DMSO) and freshly diluted in culture media for all in vitro experiments. The control cells were treated with the same amount of vehicle alone. The final DMSO concentration never exceeded 0.1% (v/v), in either control or treated samples. 3-(4,5-Dimethylthiazol-2-yl)-2,5-diphenyltetrazolium bro-mide (MTT), Hoechst33258, caffeine and propidium iodide (PI) and 5-bromo-4-chloro-3-indolyl-phosphate/nitro blue tetrazolium (BCIP/NBT) were from Sigma Chemical Co. (St. Louis, MO); human reactive monoclonal antibodies anti-p53, anti-E2F1, anti-p73, anti-Apaf-1, anti- HDM2, anti-γH2AX, anti-β-actin were from Santa Cruz Biotechno logy (Santa Cruz, CA) and human anti-NF-κB, anti-cyclinB1, anti-CDK1, anti-p21 $^{Cip1/WAF1}$, anti-cleaved PARP-1, anti-Bax, anti-Bcl-2, anti-caspase-3 were from Cell signaling Technology (Beverly, MA).

CELL LINES AND CELL CULTURE

The human cell lines used included: K562 human Chronic Myeloid Leukemia cells, Hela cervix carcinoma cells, HepG2 human liver hepatocellular carcinoma cells, MCF-7 human breast carcinoma cells, HCT116 human colon cancer cells, MRC-5 human lung fibroblast cells and NRK rat kidney cells. All cells were purchased from Cell Bank of Type Culture Collection of Chinese Academy of Sciences (Shanghai, China). K562, Hela, HepG2, MCF-7, and HCT116 cells were cultured in RPMI1640 medium, supplemented with 10% heat-inactivated bovine serum, penicillin (100 U/ml) and strepto-mycin (100 U/ml). MRC-5 and NRK cells were cultured in RPMI1640 medium, supplemented with 10% heat-inactivated fetal calf serum, penicillin (100 U/ml) and streptomycin (100 U/ml). Cells were incubated at 37°C in a humidified atmosphere of 95% air and 5% CO_2.

CYTOTOXICITY ASSAY

The cytotoxicity assay was performed by MTT method [Liu et al., 2007]. The cytotoxicity of 7-d was expressed as IC_{50} (concentration of 50% cytotoxicity, which was extrapolated from linear regression analysis of experimental data).

COLONY FORMING ASSAY

Hela, MCF-7, HCT116, HepG2 cells were plated in 24-well culture plate (200–300 cells/well) respectively, and allowed to adhere for 10 h before treatment. K562 cells were plated in 24-well culture plate with culture medium and agarose mixture (according to the ratio of culture medium: agarose = 3:1). Culture medium containing 7-d ranging from 0.2 to 1 μM or without 7-d was added to cells and incubated for 6 days. After that, wells were fixed with methanol and stained with 5% Giemsa solution and colonies (>50 cells) were counted under an inverted microscope. The antiproliferation activity was expressed as EC_{50} (concentration of 50% inhibitory colony number).

COMET ASSAY

K562 cells were treated with 4 μM 7-d for 24 h, and the assay was performed according to the manufacturer's protocol (Kengen, CN). Briefly, cells were harvested, and washed in ice-cold 1× PBS. After washing, 1×10^6 cells/ml were combined with molten LMA garose (Kengen) at 37°C at a ratio of 1:8 (vol/vol). Cell mixture was spread onto a slide embedded with normal agarose and allowed to solidify at 4°C in the dark. Cells were lysed in prechilled lysis solution for 1 h, after which the cells were immersed in a freshly prepared alkaline solution (300 mM NaOH, 1 mM EDTA, pH > 13) for 20 min. The samples were then electrophoresed at 300 mA for 30 min, washed, air-dried, and stained with 20 μl PI (5 μg/ml). The slides were visualized by fluorescence microscopy (Optimas, MD). For each sample, a minimum of 50 cells were scored at 400× magnification.

FLOW CYTOMETRIC ANALYSIS OF CELLULAR DNA CONTENT

Flow cytometric analysis of cellular DNA content was performed as described previously [Wang et al., 2006]. Briefly, cells (2×10^6) were seeded in a six-well culture plate. After 12 h incubation, cells were treated with 7-d at various concentrations and for different time. Both floating and attached cells were collected and stained with PI (50 μg/ml) and analyzed in a FACScan flow cytometer (Becton Dickinson). The percentage of cells in G0/G1 phase, S phase and G2/M phase was analyzed using standard ModiFit and CellQuest software programs.

FLOW CYTOMETRIC ANALYSIS OF APOPTOSIS AND NECROSIS

Extent of apoptosis was measured through Annexin V-FITC apoptosis detection kit (Invitrogen) as described by the manufacture's instruction. Briefly, K562 cells (1×10^6/2 ml/well) were seeded in six-well plates and treated with 7-d at various concentrations or for different time. After that, cells were collected and stained with AnnexinV-FITC and PI and then analyzed by flow cytometry using FACScan flow cytometer (Becton Dickinson). The fraction of cell population in different quadrants was analyzed using quadrant statistics. Cells in the lower right quadrant represented early apoptosis and in the upper right quadrant represented late apoptotic cells [Verma et al., 2008].

FLUORESCENT MORPHOLOGICAL ASSAY

Cells from exponentially growing cultures were seeded in 24-well culture plate and treated with 4 μM 7-d for 24 h. Cells were washed with PBS, fixed in MeOH-HOAc (3:1, v/v) for 10 min at 4°C, and stained with Hoechst 33258 (5 μg/ml in PBS) for 5 min at room temperature and then examined with a LEICA DMIRB fluorescent microscope at 356 nm.

DNA FRAGMENTATION ASSAY

The isolation of fragmented DNA was carried out according to the previous procedure [Kwon et al., 2006]. Briefly, genomic DNA was extracted from 7-d treated K562 cells (0, 12, 24, and 48 h; 4 μM) and used for agarose gel analysis.

WESTERN BLOTTING ANALYSIS

7-d treated cells were subsequently lyzed in lysis buffer [20 mM Tris (pH 7.4), 25 0 mM NaCl, 2 mM EDTA (pH 8.0), 0.1% Triton X-100, 0.01 mg/ml aprotinin, 0.003 mg/ml leupeptin, 0.4 mM phenylmethylsulfonyl fluoride (PMSF), and 4 mM NaVO4]. The extraction and isolation of nuclear fraction were performed according to the method of Levites et al. [2002]. Lysates were then spun at 14,000*g* at 4°C for 10 min and supernatants were in parallel lanes on 10% sodium dodecyl sulfate (SDS) gels. After electrophoresis, the proteins were electro-transferred to a PVDF membrane, blocked with 5% nonfat milk, and probed with antibodies (1:1,000) for appropriate primary overnight at 4°C. The blot was then incubated with appropriate secondary antibody alkaline phosphatase (AP) conjugated and detected in 5 ml AP buffer containing 16.5 μl BCIP and 33 μl NBT at room temperature for 10–20 min, and then photographed. β- Actin was used as a loading control.

REAL-TIME QUANTITATIVE REVERSE TRANSCRIPTION-PCR ANALYSIS

Total RNA of 7-d-treated cells was extracted using TRIZOL™ reagent (Promega Corporation) according to the supplier's instruction. RNA was quantitated by optical density measurement at 260 and 280 nm using a spectrophotometer (all RNA samples had an A260/A280 ratio >1.8), and integrity was confirmed by running RNA on a 1.2% agarose gel. Reverse transcription was performed with 1 μg of total RNA using Reverse Transcription System (Takara Shuzo, Shiga, Japan). Real-time PCR was performed using SYBR Green Supermix with an iCycler® thermal cycler (Bio-Rad). Primers were obtained from Shanghai Sangon Biological Engineering Technology & Services Co. Ltd. (Shanghai, China) and their sequences were shown in Supplementary Table 1. The data were collected and analyzed with the comparative Ct (threshold cycle) method using GADPH as the reference gene.

COIMMUNOPRECIPITATION ASSAY

Coimmunoprecipitation was conducted as described previously [Liang et al., 2010]. In brief, cells were collected and lysed in 1 ml of immunoprecipitation lysis buffer (300 mmol/L of NaCl, 50 mmol/L of Tris-Cl, pH 7.6, 0.5% Triton X-100, protease inhibitors, 10 mmol/L of Na4P2O7, 1 mmol/L of Na_3VO_4, 25 mmol/L of NaF, and 1 mmol/L of b-glycerophosphate). Protein concentrations of cell lysates were determined using the Bradford method, and 500 μg of protein was precleared and then incubated with HDM2 antibody in extraction buffer at 4°C overnight. The immune complexes were precipitated with protein A/G agarose beads (Sigma) for 2 h and washed five times with extraction buffer before boiling in SDS sample buffer.

Immunoprecipitated proteins were separated by SDS–PAGE, and Western blot analysis was carried out as described earlier.

RNA INTERFERENCE ASSAY

The cells were plated at 5×10^5 cells/ml in a six-well plate. Twenty-four hours after plating, the cells were transfected with the E2F1 siRNA. The scrambled siRNA oligonucleotides used as a control for E2F1 RNA interference experiments. Their sequences were in Supplementary Table 1. The transfection of the siRNA was carried out according to the Lipofectamine™ RNAiMAX transfection Reagents guidelines (Invitrogen). Subsequently, the cells were collected and analyzed using flow cytometry and western blotting.

STATISTICAL ANALYSIS

Each experimental value was expressed as means ± standard deviation (SD). Significant differences between experimental groups and control were determined using the unpaired Student's *t*-test. Statistical analysis was performed using the Origin 7.5 software to evaluate the significance of differences. In all cases, $P < 0.05$ was considered significant.

RESULTS

EFFECTS OF 7-d ON CELL VIABILITY IN HUMAN CANCER CELL LINES AND NORMAL CELL LINES

To investigate the potential anticancer activity of 7-d in human cancer cells, we first examined the effect of 7-d on cell viability in five human cancer cell lines. As shown in Supplementary Figure 1A and 1B. 7-d seemed to be more potent than amonafide against Hela, HepG2, HCT116, MCF-7, K562, with the IC_{50} values of 4.68, 8.45, 3.89, 4.56, and 4.29 μM, respectively, all below the responding values of amonafide (11.56, 43.1, 50, 27.4, and 13.1 μM, respectively. However, at these concentrations, 7-d had less effect on the cell viability of normal MRC-5 and NRK cells. In addition, 7-d resulted in a significant inhibition of colony formation of five cancer cell lines compared with control (Supplementary Fig 1C). The EC_{50} values on colony formation were showed in Table I. When counting up above-mentioned results, therapeutic index (the ratio of IC_{50} VS. EC_{50}) for these five cancer cell lines showed the following order: K562 > MCF-7 > HepG2 > Hela > HCT116. It showed that p53-deficient K562 cells were sensitive to 7-d with the highest therapeutic index equal to 11.59 (Table I). We further evaluate the toxicity effect of 7-d on K562 cells by the MTT assay. Supplementary Figure 1D demonstrated that 7-d inhibited cellular viability in a time-and dose-dependent manner. The viability of K562 cells was reduced to 50% upon a 48 h exposure to 2.16 μM 7-d and a 60 h exposure to 1.85 μM 7-d.

TABLE I. Growth Inhibition Effect of 7-d on Five Established Cell Lines

	K562	HepG2	MCF-7	HCT116	Hela
IC50(μM)	4.29 ± 0.83	8.45 ± 0.13	4.56 ± 0.86	3.89 ± 0.15	4.68 ± 0.56
EC50(μM)	0.37 ± 0.08	0.84 ± 0.11	0.4 ± 0.03	0.78 ± 0.15	0.54 ± 0.04
TI	11.59	10.06	11.4	4.99	8.67

Each value represented means ± standard deviation (SD) of three independent experiments. Therapeutic index (TI) was equal to the ratio of IC_{50} vs. EC_{50}.

EFFECTS OF 7-d ON CELL CYCLE PROGRESSION IN K562 CELLS

In this study we analyzed the cell cycle to characterize the inhibition of K562 cell growth induced by 7-d and to relate this to cell cycle progression. Compared with the control treatment, 7-d could cause an appreciable arrest in the G2/M phase in dose- and time-dependent manner (Fig. 2A,B). Cells separately treated with 0, 1, 2, or 4 μM of 7-d for 24 h resulted in the accumulation of G2/M phase, from 12.05 to 67.63% (Fig. 2A). Furthermore, as shown in Fig. 2B, the K562 cell population gradually increased from 12.44% at 0 h to 28.1% after 24 h and 61.89% after 48 h in the G2/M phase.

MODE OF 7-d–INDUCED CELL DEATH IN K562 CELLS

In order to identify the mode of K562 cell death (apoptosis or necrosis) following 7-d treatment, a combination of PI and Annexin V staining and FACS analysis was used. After K562 cells were incubated with various concentrations of 7-d for 24 h or 2 μM 7-d for different time. Cells were stained with AnnexinV-FITC and PI which could assess the early apoptotic and laten apoptotic cell population. 7-d produced a dose- and time-dependent increase in the apoptotic cell population. The apoptotic population in the untreated cell was 4.84%, which increased to 84.31% at 4 μM (Fig. 3A). Also cells separately treated with 2 μM 7-d for 0, 12, 24, and 48 h resulted in the accumulation of apoptotic population, from 3.06% at 0 h to 97.78% after 48 h (Fig. 3B). Next, we further confirmed the above results by fluorescent dye Hoechst 33258 staining and DNA fragmentation assay. Figure 3C showed both control cells were normal and the nuclei were round and homogeneous, while the cells treated with 7-d at 4 μM exhibited the characteristics of apoptosis along with cell shrinkage, nuclear condensation and apoptotic bodies. As shown in Figure 3D, exposure of cells to 7-d (0, 12, 24, and 48 h) at 4 μM led to evident DNA fragmentation as indicated by the formation of DNA ladder.

EFFECT OF 7-d ON CELL CYCLE REGULATORY MOLECULES IN K562 CELLS

It has been well documented that the cell cycle is primarily regulated by complexes containing CDKs and the Cyclins. Regulation of CyclinB1/Cdk1 complexes at multiple levels ensures the tight control G2/M transition. $P21^{Cip1/WAF1}$, a Cyclin-dependent kinase inhibitor, is known for its ability to be up-regulated by p53, both of which are integrated in G1 and G2 arrest machinery in response to DNA damage [Ko et al., 2005; Chiu et al., 2009]. To further investigate the molecular changes involved in 7-d-mediated G2/M cell cycle arrest in p53-deficient K562 cells, we analyzed whether 7-d treatment altered the expression of $p21^{Cip1/WAF1}$, Cdk1, and CyclinB1. As shown in Figure 4A, treatment of K562 cells with 0, 1, 2, 4, and 5 μM of 7-d for 24 h increased $p21^{Cip1/WAF1}$ and CyclinB1 in a concentration-dependent manner, however, Cdk1 kept unchanged from the beginning to the end. The results indicated that treatment of K562 cells with 7-d activated $p21^{Cip1/WAF1}$ in a p53 independent manner. Then, accumulation of $p21^{Cip1/WAF1}$ inhibited

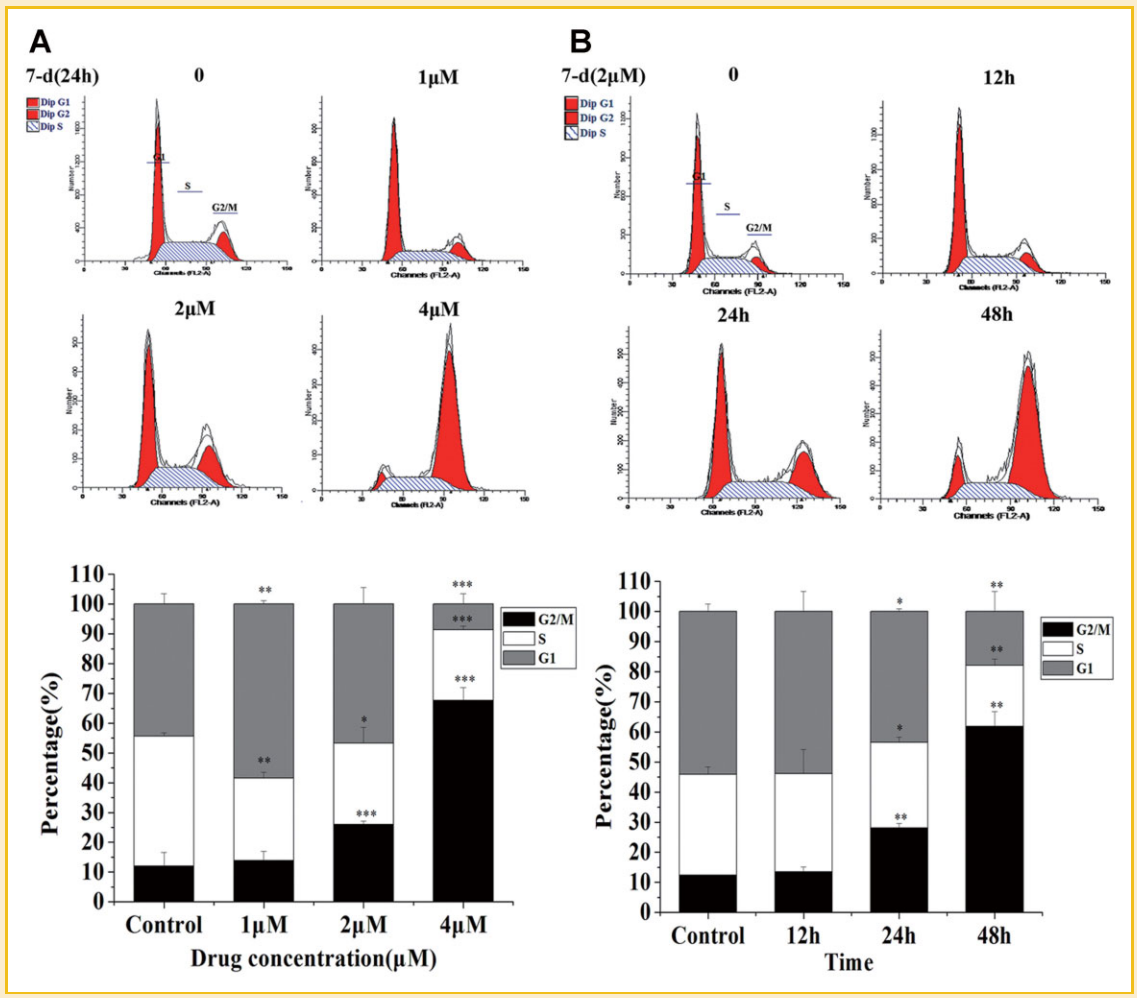

Fig. 2. Dose- and time-dependent effects of 7-d on cell cycle distribution in K562 cells. K562 cells (1×10^6/1 ml/6-well plates) were incubated with 0, 1, or 2 μM 7-d for 24 h and treated with 7-d (2 μM) for 0, 24, and 48 h, respectively. Cell cycle analysis was then conducted using flow cytometry as described in the Materials and Methods section. A: Concentration-dependent G2/M arrest by 7-d. B: Time-dependent G2/M arrest by 7-d. Experiments were repeated independently three times with similar results. The data shown are results of a representative experiment. Cell cycle distribution histograms were expressed as means ± SD of three independent experiments. The values indicated the percentage of cells in the indicated phases of the cell cycle. Significant differences from control were indicated by $^{*}P < 0.05$; $^{**}P < 0.01$; $^{***}P < 0.001$. [Color figure can be seen in the online version of this article, available at http://wileyonlinelibrary.com/journal/jcb]

the expression of cyclin-dependent kinases, such as CyclinB1 and Cdk1.

EFFECT OF 7-d ON APOPTOSIS REGULATORY MOLECULES IN K562 CELLS

The transcription factor NF-κB has antiapoptotic properties and may confer chemoresistance to cancer [Lin et al., 2010]. Members of the Bcl-2 family proteins are associated with the mitochondrial membrane and regulate membrane integrity. The balance between the expression levels of the protein units (e.g., Bcl-2 and Bax) is critical for cell survival or death. The Bcl-2/Bax ratio might contribute to apoptosis via caspases activation in the mitochondria pathway [Ghobrial et al., 2005]. Therefore, to understand the ultimate molecular events involved in 7-d-induced cell apoptosis, we next investigated the effect of the 7-d on nuclear translocation of NF-κB, Bax/Bcl-2 ratio, executioner caspase-3 and its substrate cleaved PARP-1 expression level. K562 cells were treated with 0, 1, 2, 4, and 5 μM 7-d for 24 h, respectively. The result showed that nuclear translocation of NF-κB was suppressed (Fig. 4B). Meanwhile up-regulation of Bax and down-regulation of Bcl-2 were observed, suggesting an increase of Bax/Bcl-2 ratios which might be involved in apoptosis induced by 7-d. Furthermore, 7-d caused caspase-3 activation and cleavage of a well-known substrate of activated caspase (poly (ADP-ribose) polymerase-1 (PARP-1)) which in involved in apoptotic signaling (Fig. 4B).

7-d TREATMENT TRIGGERED ATM/ATR-DEPENDENT DNA DAMAGE SIGNALING

To evaluate whether 7-d causes DNA damage, we used the alkaline version of the comet assay to detect a variety of DNA damage [Olive and Banath, 2006]. K562 cells were treated with 4 μM 7-d for 24 h. As shown in Figure 5A, significantly comet migration was observed.

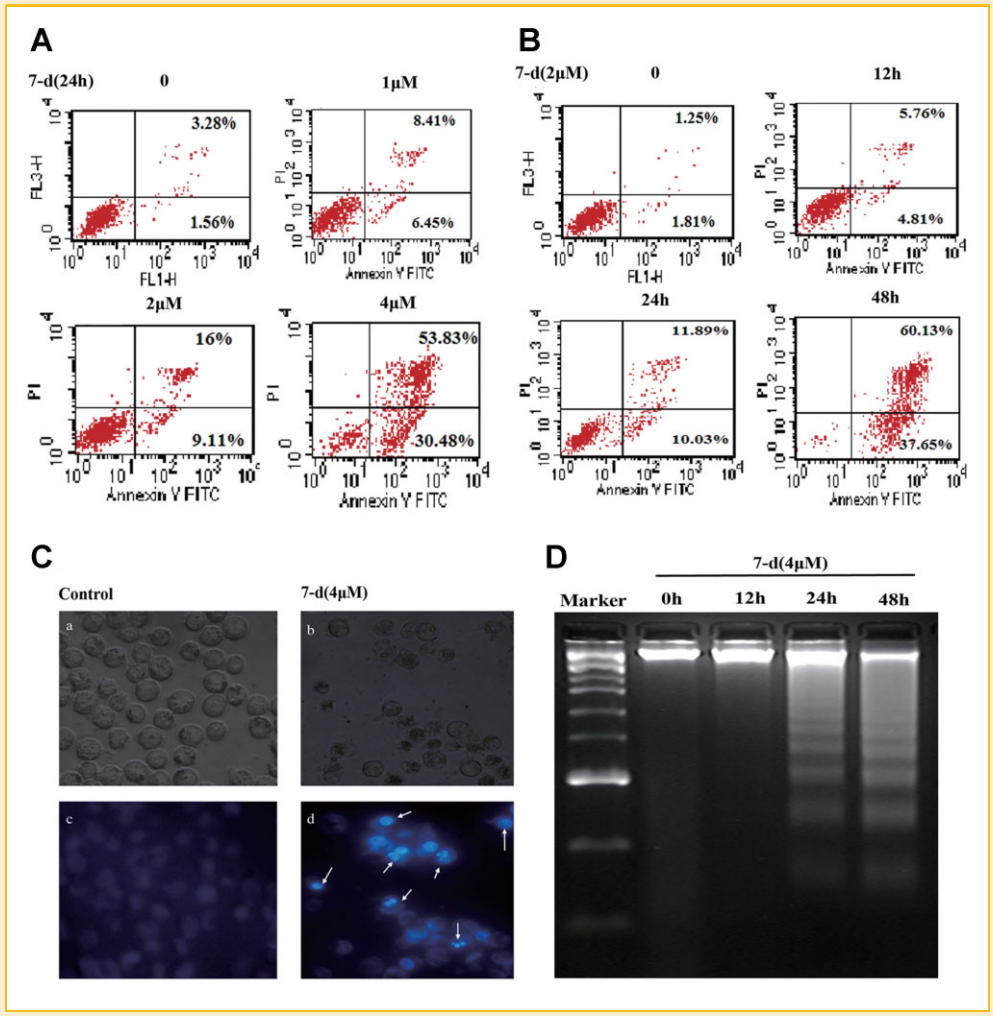

Fig. 3. Flow cytometric analysis of 7-d-induced apoptosis in K562 cells using Annexin V-FITC/PI. K562 Cells (1×10^6/1 ml/6-well plates) were incubated with 0, 1, or 2 μM 7-d for 24 h and treated with 7-d (2 μM) for 0, 24 and 48 h, respectively, subsequently stained with Annexin V-FITC/PI to analyze apoptotic and necrotic cell populations. Cells in the lower right quadrant represented early apoptosis and cells in the upper right quadrant represented late apoptosis. A: Dose-dependent apoptosis by 7-d treatment. B: Time-dependent apoptosis by 7-d treatment. Data are representative of one of three similar experiments. C: Examples of the cellular morphology. K562 cells were treated with 4 μM 7-d for 24 h, and then visualized by phase contrast microscope and LEICA fluorescence microscope, respectively. Condensed and fragmented nuclei and apoptotic bodies (arrows) were seen in the 7-d -treated cells (d), but not in the control (c). D: DNA fragmentation of K562 cells exposed to 7-d. K562 cells were incubated with 4 μM of 7-d for 0, 12, 24, and 48 h. DNA ladders reflecting the presence of DNA fragments were viewed on ethidiumbromide-stained gel. Experiments were repeated independently three times with similar results. Typical result from three independent experiments was shown. [Color figure can be seen in the online version of this article, available at http://wileyonlinelibrary.com/journal/jcb]

Quantitative analysis of comet assay results showed that the tail moments of 7-d-treated cells were significantly different from those of the controls. In parallel, western blotting assay showed that the phosphorylation of histone H2AX at Ser139, a marker of DNA Double strand breaks (DSB) [Kuo and Yang, 2008], dramatically increased in a time-dependent way within 8 h (Fig. 5B). This result suggested that 7-d can induce significant DNA DSB in K562 cells in the early stage. Ataxia-telangiectasia-mutated (ATM) and ATM-and Rad3-related (ATR) kinases are two members of phosphatidylinositol-3-kinase-related kinase family playing important roles in sensing DNA damage. Histone H2AX Serine 139, named γ-H2AX, is also an early phosphorylated target of ATM. Caffeine, an ATM/ATR kinase inhibitor [Sarkaria et al., 1999], was used to examine whether ATM/ATR signaling pathway was activated in the 7-d-induced DNA damage response. As shown in Figure 5B, preincubation with 5 mM caffeine for 1 h downregulated 7-d-induced expression of γ-H2AX, confirming that ATM/ATR pathway participated in 7-d-induced DNA damage response.

CAFFEINE ANTAGONIZES 7-d-INDUCED G2/M ARREST AND APOPTOSIS

To directly examine whether cell cycle arrest and apoptosis induced by 7-d treatment was associated with its DNA damage response. The ATM/ATR inhibitor Caffeine was used to clarify the role of ATM and/or ATR in the 7-d-induced G2-M arrest in K562 cells. As shown in Figure 5C,D, 1 h pretreatment of caffeine at 5 mM significantly

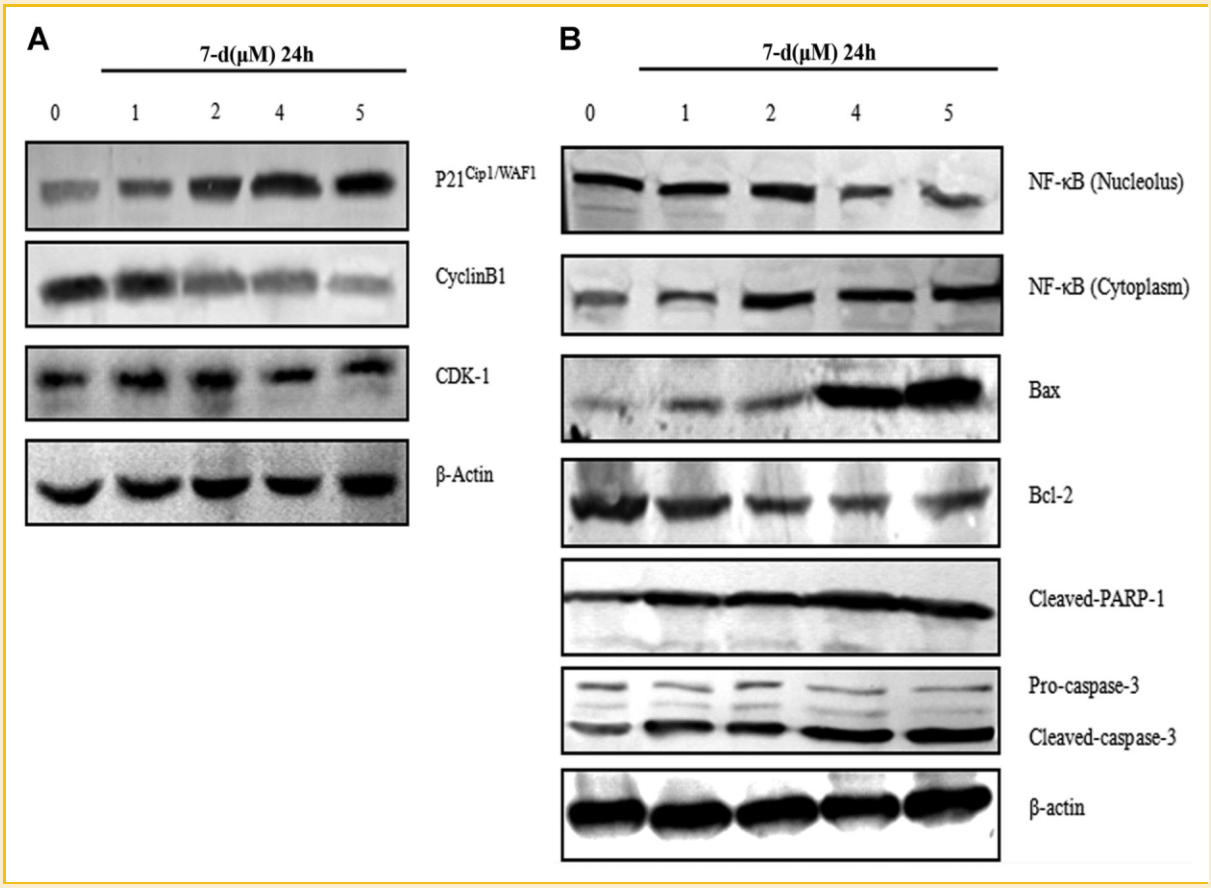

Fig. 4. Effects of 7-d on cell cycle regulatory proteins and apoptosis regulatory molecules in K562 cells. Proteins from K562 cells treated with 7-d (24 h) for 0, 1, 2, 4, and 5 μM were analyzed using western blotting. A: Total protein extracts were prepared after treatment for 24 h, and analyzed with antibodies to $p21^{Cip1/WAF1}$, Cyclin B1, and CDK1. B: Total protein and nuclear extracts were prepared after treatment for 24 h, and analyzed with antibodies to NF-κB, Bax, Bcl-2, caspase-3, and cleavaged-PARP-1. β-actin was used as a loading control. Western blots were representative of three independent experiments.

abated 7-d-induced G2/M arrest and apoptosis, suggesting that G2/M arrest and apoptosis of K562 cells were caused by DSBs, which were sensed by ATM and/or ATR.

EFFECT OF 7-d ON p53, E2F1, p73, HDM2, AND Apaf-1 EXPRESSION

On account of E2F1 can trigger cell death in p53-deficient tumors, including most leukemia cell lines [Fueyo et al., 1998]. We therefore examined whether E2F1 and its target gene p73, Apaf-1, HDM2 were involved in 7-d-induced DNA damage, G2/M arrest and apoptosis in K562 cells. Western blot was used to assess E2F1, p73, p53, HDM2 and Apaf-1 protein expression levels in K562 cells which were treated with 0, 1, 2, 4, and 5 μM for 24 h. Figure 6A represented a typical western blot result of increase in the level of E2F1, p73, and Apaf-1 proteins were observed. Consistent with previous reports, wild-p53 protein in either control or 7-d treated K562 cells were unable to be detected. A time course study with 2 μM of 7-d showed that protein levels of E2F1, p73, and Apaf-1 increased after 24 h, which intensified with time (Fig. 6B). These results demonstrated that 7-d-induced expression of E2F1, p73, and Apaf-1 is dose and time dependent. Intriguingly, no detectable increase expression levels of HDM2 were observed in 7-d treated K562 cells (Fig. 6A,B). We had determined that 7-d could cause a change in the protein level of E2F1, p73, Apaf-1 except p53 and then we examined the mRNA levels by Real-Time Quantitative RT-PCR analysis. In accordance with above protein levels change, the results indicated that the mRNA expression of E2F1, p73, and Apaf-1 increased in a time-dependent manner. However, the mRNA level of p53 in the K562 cells treated with 7-d kept unchanged in comparison with control cells (Fig. 6C).

7-d PREVENTS THE PHYSICAL INTERACTION BETWEEN HDM2 AND p73 IN K562 CELLS

It has been reported that HDM2, a key negative regulator of p53, also binds to and inhibits p73 transcriptional activity [Lu et al., 1999]. We therefore asked whether 7-d could disrupt p73 binding to HDM2. The Co-immunoprecipitation assay was performed to confirm our hypothesis that 7-d-induced p73 accumulation was accompanied by the dissociation of the HDM2-p73 complex. As shown in Figure 6D, 7-d caused p73 dissociation from HDM2 in response to 4 μM at 24 h.

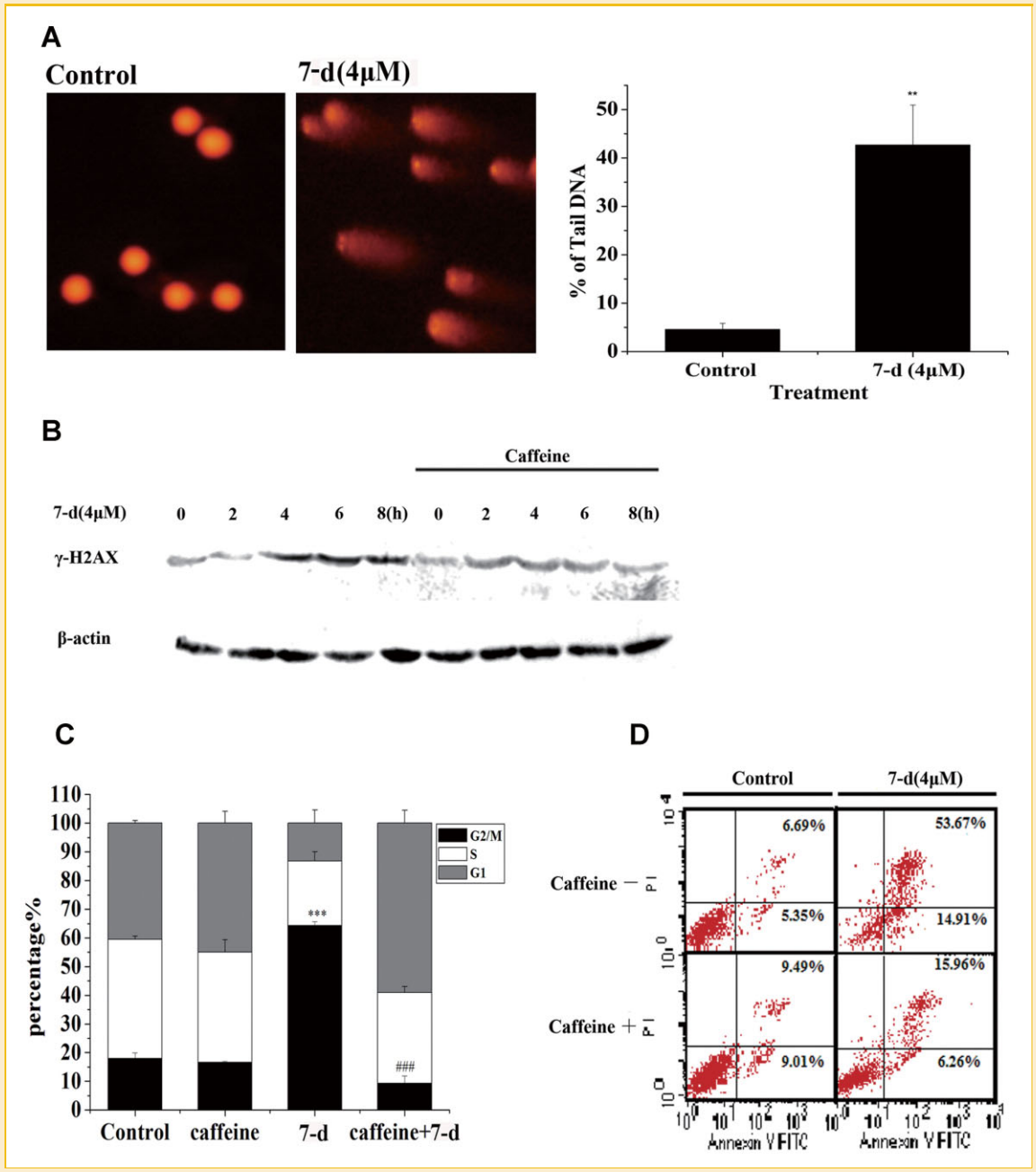

Fig. 5. DNA damage signaling is triggered by 7-d treatments and subsequently mediated G2-M arrest and apoptosis in K562 cells. A: Detecting DNA damage in individual cells by comet assay. K562 cells were treated with 4 μM 7-d for 24 h and then subjected to an analysis by comet assay. Typical "comet pattern" of damaged DNA was visualized by a fluorescent microscope. Semiquantitative analysis of the results presented in (A), expressed as the average of % tail DNA analyzed by the CometScore™ software. More than 50 cells were scored in each condition. Significant difference of 7-d treatment from the control were indicated by $^{**}P < 0.01$. B: Western blotting analyses of H2AX-P^{Ser139}. K562 cells were un-pretreated or pretreated with 5 mM caffeine for 1 h, and then treated with 4 μM 7-d for 0, 2, 4, 6, and 8 h. Phosphorylated H2AX-P^{Ser139} levels were analyzed by western blotting. C,D): ATM/ATR inhibitor caffeine (5 mM) abrogated 7-d -induced G2/M arrest and apoptosis. K562 cells were pretreated with 5 mM caffeine for 1 h, following with 4 μM 7-d for 24 h, then analyzed by FACS for cell cycle distribution and apoptosis. Experiments were repeated independently three times with similar results. The data were shown are results of a representative experiment. All data were presented as the mean ± SD of three parallel samples in each team. As for G2/M cycle phase, significantly differences between control and 7-d group were indicated by $^{***}P < 0.001$; between 7-d group and caffeine + 7-d group were indicated by $^{\#\#\#}P < 0.001$. [Color figure can be seen in the online version of this article, available at http://wileyonlinelibrary.com/journal/jcb]

INHIBITION OF 7-d-INDUCED CELL CYCLE ARREST AND APOPTOSIS BY KNOCKOUT OF E2F1 USING siRNA TRANSFECTION

To directly address the role of E2F1 in 7-d-induced cell cycle arrest and apoptosis, the siRNA technique was used to selectively knock down the E2F1 gene. Western blot analysis was used to confirm that E2F1siRNA, but not control siRNA was able to reduce E2F1 protein expression (Fig. 7A). When the K562 cells were transfected with siRNA of E2F1, then treated with 2 μM 7-d for 48 h, the apoptotic

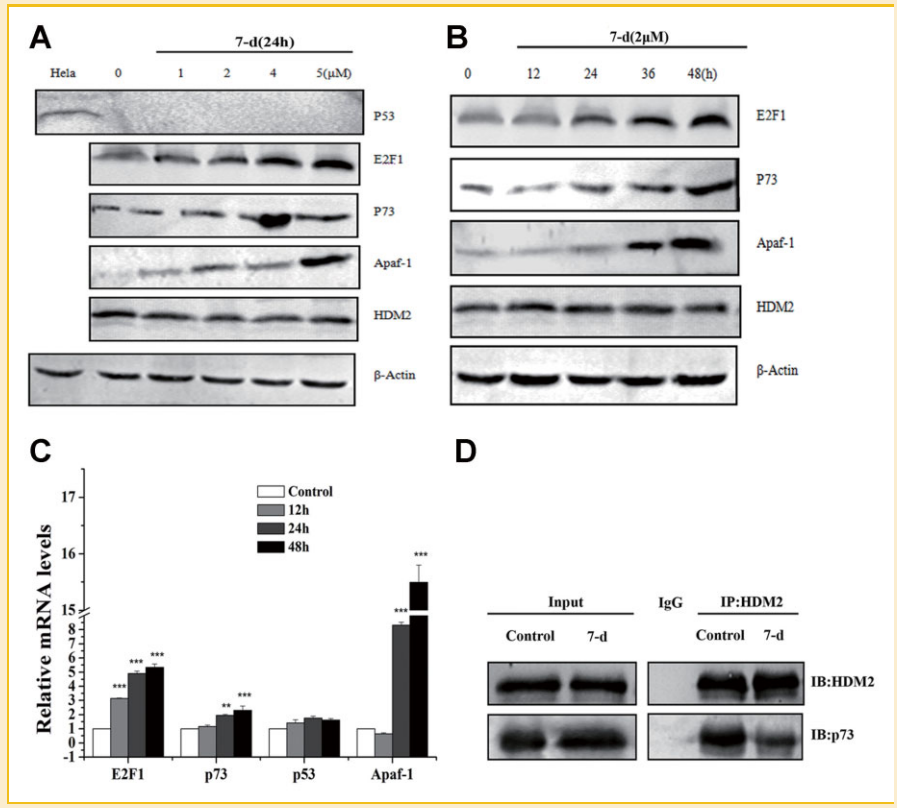

Fig. 6. 7-d treatment increased the protein and mRNA expression of E2F1, p73, Apaf-1 and disrupted endogenous p73-HDM2 binding. Western blot analysis of protein extracts obtained from K562 cells were treated with 0, 1, 2, 4, and 5 μM 7-d for 24 h and 7-d (2 μM) for 12, 24, 36, and 48 h, respectively. A: Total protein extracts were prepared with the indicated concentration of 7-d for 24 h. B: Total protein extracts were prepared with 2 μM 7-d for the indicated time. Total protein extracts of A and B were then analyzed with antibodies to HDM2, E2F1, p73, Apaf-1, and/or p53. p53 in Hela used as a positive control for wild-p53. β-actin was used as a loading control. C: Effect of 7-d on mRNA expression of E2F1, p73, p53, Apaf-1 genes in K562 cells. Cells were treated with 2 μM 7-d for 0, 12, 24, 48 h and then harvested. Quantification real-time reverse transcription-PCR was done on cDNA by using $2^{-\triangle\triangle CT}$ method according to quantitative real-time RT-PCR. D: Disruption of endogenous p73-HDM2 binding by 7-d. K562 cells were treated with 4 μM for 24 h. K562 lysates were immunoprecipitated (IP) with HDM2 or mouse immunoglobulin G (IgG) antibody, followed by immunoblotting with HDM2 and p73 antibodies. Western blots were representative of three independent experiments. QRT-PCR data were presented as means ± SD and as representative of an average of three independent experiments per concentration. Significant differences from control were indicated by $^{*}P < 0.05$; $^{**}P < 0.01$; $^{***}P < 0.001$

induction was decreased by 59% and the effect of 7-d on G2/M accumulation was reduced by 40% compared to that without siRNA transfection (Fig. 7B,C). Furthermore, the levels of p73, Apaf-1, and p21 $^{Cip1/WAF1}$ in K562 cells transfected with E2F1 siRNA were significantly decreased by 70–80%, as demonstrated using western blotting (Fig. 7D). Accordingly, these data demonstrated the involvement of E2F1-dependent pathway in 7-d-induced cell cycle arrest and apoptosis in K562 cells.

DISCUSSION

As we know, amonafide is a traditional Topoisomerase II-targeted drug. In our previous study, a novel amonafide analogue 7-d was designed to aim at improving the antitumor efficiency and in particular, to alleviate the toxicity of the parent compound amonafide [Chen et al., 2010]. In the course of investigating the antitumor activities of 7-d, K562, a congenital p53 deficient human myeloid leukemia cell line [Law et al., 1993], seemed to be more sensitive to 7-d. So it was of interest to further investigate the mechanism underlying the effects of 7-d-induced in human CML K562 cells lack of p53.

MTT and colony forming assay revealed that 7-d could cause more toxicity on a panel of established cancer cell lines (Hela, HepG2, MCF-7, HCT116, K562), than amonafide with the IC_{50} values all below the responding values of amonafide. Meanwhile, we were happy to find that cytotoxicity of 7-d on normal cells MRC-5 and NRK was much lower than human cancer cells (Supplementary Fig. 1A). The above results supported that the structure optimization of 7-d enhanced its effective and selective cytotoxicity in tumor cells. Our results also showed that K562 (p53-deficient) human Chronic Myeloid Leukemia cell was the most impressionable cancer cell to 7-d treatment, with the highest TI (IC_{50}/EC_{50}) values 11.59 (Table I). Further study on the antiproliferation effects of 7-d on K562 cells demonstrated that 7-d inhibited K562 cells growth in a time- and dose-dependent manner.

Besides, we found that the antiproliferation effects of 7-d in K562 cells could be explained by the cell cycle arrest and apoptosis. Flow cytometric analysis showed treatment of cells with 7-d not only led to G2/M arrest but also increased apoptotic cells in a dose-

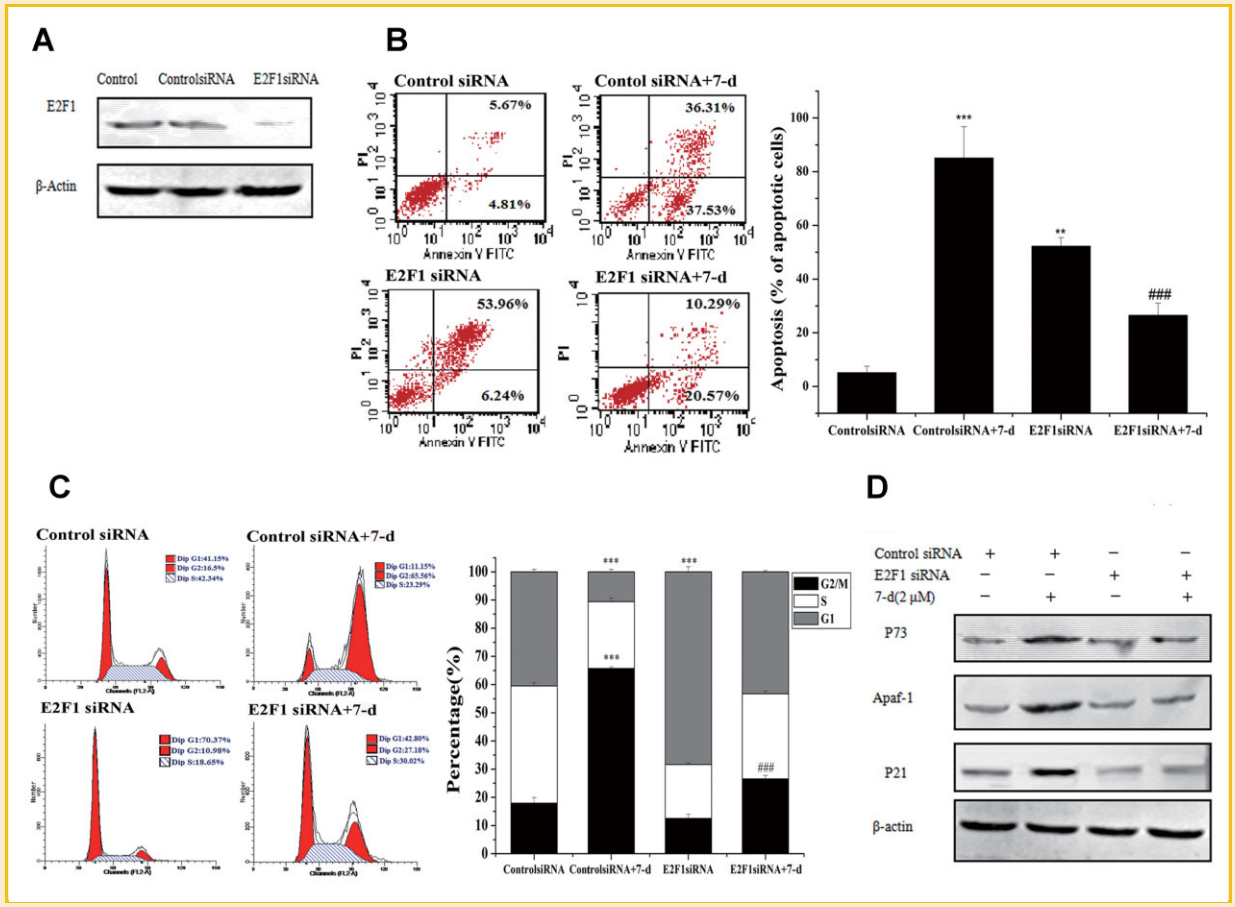

Fig. 7. Inhibition of 7-d-induced cell cycle arrest and apoptosis by transfection of E2F1 siRNA to K562 cells. The cells were transfected with a control and E2F1 siRNA duplex for 48 h plus recovery, followed by treatment with 2 μM 7-d for 48 h. A: K562 cells were transfected with Control siRNA and E2F1 siRNA, then detected by western blot. B: Apoptosis assessed using Annexin V-FITC and PI staining with flow cytometry, data are expressed as the mean ± SD, $^{**}P < 0.01$, $^{***}P < 0.001$ compared E2F1siRNA, control siRNA + 7-d, with control siRNA group; $^{###}P < 0.001$ compared E2F1 siRNA + 7-d group with control siRNA + 7-d group. C: Cell cycle distributions assessed using propidium iodide (PI) staining with flow cytometry. Cell cycle distribution histograms were presented as means ± SD of three independent experiments. As for G1 and G2/M phase, significantly differences between control siRNA + 7-d, E2F1 siRNA and control siRNA group were indicated by $^{***}P < 0.001$; significant differences between E2F1 siRNA + 7-d and control siRNA + 7-d group in G2/M phase were indicated by $^{###}P < 0.001$ (D): p73, Apaf-1, and $p21^{Cip1/WAF1}$ protein levels checked based on western blot analysis. Western blots were representative of three independent experiments. [Color figure can be seen in the online version of this article, available at http://wileyonlinelibrary.com/journal/jcb]

and time-dependent manner, meanwhile, morphological changes and formation of DNA fragmentation of K562 cells in response to 7-d treatment came to the conclusion that apoptosis was the prime cell death way related to 7-d (Figs. 2 and 3). Next, our further molecular mechanism research revealed that 7-d-induced G2/M arrest at the G2/M checkpoint of the cell cycle was related to p53-independent transcriptional up-regulation of $p21^{Cip1/WAF1}$, and down-regulating the intracellular levels of cyclinB1, without changing the levels of Cdk1 (Fig. 4A). Moreover, NF-κB nuclear localization suppression and mitochondrial death pathways were deeply responsible for the apoptotic effect of 7-d in K562 cells (Fig. 4B).

Our previous report showed 7-d could inhibit Topoisomerase II [Chen et al., 2010], which reminded us DNA damage signaling may be involved in 7-d-induced G2/M arrest and apoptosis. In the present study, we first investigated its DNA damage effects in K562 cells. Our observation suggested that 7-d could induce significant DSB in K562 cells. ATM and ATR, members of the phosphatidylinositol-3 kinases-related protein family, are two key important DNA damage sensors in response to DNA damage, particularly DSB formation [Kitagawa and Kastan, 2005]. Our data demonstrated that pretreatment of caffeine, the ATM/ATR inhibitor, abated H2AX-ser139 phosphorylation within 8 h and antagonized 7-d-induced G2-M arrest and apoptosis (Fig. 5B–D), suggesting that ATM/ATR signaling was activated in the early stage and mediated 7-d-induced cell cycle arrest and apoptosis. ATM and/or ATR kinases can initiate activation of downstream pathways through phosphorylation of targets at the site of DNA damage, especially p53, which subsequent mediates cell cycle arrest and apoptosis [Kurz and Lees-Miller, 2004; Kitagawa and Kastan, 2005]. Considering the action of 7-d in inducing cell cycle arrest and apoptosis in p53-deficient K562 cells is not dependent on p53, to further elucidate p53-independent pathway is clearly necessary.

E2F1, the first member of the E2F transcription factor family, is well known for its pivotal role in coordinating progress through the cell cycle predominantly at the G1 to S phase transition [Gorgoulis

and Tsantoulis, 2005]. Despite the clear importance of E2F1 in allowing cell-cycle progression, its another unique role in triggering cell cycle checkpoints and apoptosis in responding to DNA damage has instigated a number of studies in search of its function [Wu et al., 2009]. Some reports showed that E2F1 can be induced and phosphorylated by DNA damage responsive protein kinases, ATM and/or ATR, in a manner analogous to that of p53, which leads to its accumulation and the induction of cell cycle arrest and apoptosis [La Thangue and Stevens, 2004; Carcagno et al., 2009]. The accumulation of E2F1 can lead cell death through p53-dependent and p53-independent pathways [Ginsberg, 2002; Stanelle and Putzer, 2006]. In cell types lacking p53, E2F1 become an effective death-inducer to activate many apoptosis genes not directly related to p53 pathway. The p53 family member p73 and Apoptosis protease-activating factor 1 (Apaf-1), has been described as two key downstream targets mediating E2F1-induce apoptosis. Activation of p73 in turn triggers the activation of p53-responsive target genes, such as Bax, Noxa, Puma, etc. and leads to apoptosis, Apaf-1 in turn complexes with cytochrome *c* released from mitochondria, activating a cascade of caspases [Furukawa et al., 2002]. In addition to the well-studied p73 and Apaf-1, E2F1 may also transcriptionally induce other pro-apoptotic genes, including BH3 proteins, caspase family members etc. and inhibit survival or antiapoptotic members, such as NF-κB and antiapoptotic Bcl-2 family members [Hershko and Ginsberg, 2004]. In our current study, both protein and mRNA levels of E2F1, p73, and Apaf-1 were increased in K562 cells (Fig. 6). Moreover, the depletion of E2F1 expression resulted in a significant decrease of apoptosis induction (Fig. 7B,C) and inhibition of the cellular level of p73 and Apaf-1 expression (Fig. 7D) in K562 cells treated with 7-d when compared with control cells, indicating the direct involvement of two major E2F1-dependent p73 and Apaf-1 pathways in the 7-d-induced cell apoptosis.

HDM2 has been found to be overexpressed in approximately 50% leukemias. Inactivation of wild-type p53 frequently occurs through binding to its principal cellular regulator HDM2 [Kojima et al., 2005]. Lau et al. [2008] reported that HDM2 also binds to and inhibits p73 activity. As Figure 6A,B shown, the protein expression levels of HDM2 were unchanged in response to 7-d treatment all the time. However, Co-IP assay revealed that 7-d-induced p73 expression is accompanied by the dissociation of the HDM2/p73 complex at the post-translational level (Fig. 6D). We do not yet know the exact underlying mechanisms. But the HDM2-p73-P14ARF pathway had been shown to be related to some tumor progression [Schlott et al., 2004]. Besides, E2F1 was reported to prevent HDM2 binding to p53 to proteosomal degradation via the direct transactivation p14ARF tumor suppressor gene [Pomerantz et al., 1998], so we hypothesized that in a situation where HDM2 is overexpressed. In order to promise cells undergoing cell cycle arrest and apoptosis under genotoxic pressure, E2F1 may augment dissociation of HDM2 and p73 too. Of course, this hypothesis needs further investigation.

On the other hand, silencing E2F1 could obviously reduce the effects of 7-d on G2/M accumulation and decrease of p21 $^{Cip1/WAF1}$ expression too (Fig. 7D). So far, few studies reported E2F1 can directly upregulate p21 $^{Cip1/WAF1}$, but previous studies revealed that p73 can substitute p53 to activate its target gene p21 $^{Cip1/WAF1}$ in the absence of p53 [Goldschneider et al., 2004]. So, we thought p21 $^{Cip1/WAF1}$ is regulated by p73 but not directly by E2F1 in this process, which in turn inhibited CyclinB1/Cdk2 complexes, resulted in the G2/M arrest in K562 cells. Taken together, these data suggested that the E2F1/p73/p21 $^{Cip1/WAF1}$ pathway should partially responsible for 7-d-induced G2/M arrest. Meanwhile, in Figure 7, we observed that knockout of E2F1 itself could also increase the apoptotic cell number and G1/S phase in K562 cells. One rational explanation is that under normal conditions, E2F1 keeps its central modulator roles of the G1 to S-phase progression in K562 cells; after 7-d induced DSB, which could soon switch to an onco-suppressor role. Liontos et al. [2009] reported that the ability of E2F1 to trigger both proliferation and apoptosis seems not paradoxical, because the cell could consume less time and energy to control the switch from the proliferation state to the self-destruction program in case of irreversible cellular damage.

In conclusion, our present study demonstrated proposed working model of 7-d -induced G2/M arrest and apoptosis in K562 cells (Fig. 8). 7-d induced DNA DSB in K562 cells, at the same time, ATM and/or ATR DNA damage signaling sensed the DSB and subsequently activated E2F1 expression. Up-regulation of E2F1 leads to activation of two major E2F1-dependent pathways: E2F1/p73 and E2F1/Apaf-1 signaling pathways. Activation of p73, Apaf-1 or E2F1 itself led to the intrinsic apoptotic pathway, on the other hand, p73 activate p21 $^{Cip1/WAF1}$, which downregulated CyclinB1, ultimately resulted G2/M arrest. To our knowledge, this is the first report to provide proof of the mechanistic basis that 7-d induced cell cycle arrest and apoptosis in K562 cells via E2F1 signal pathways.

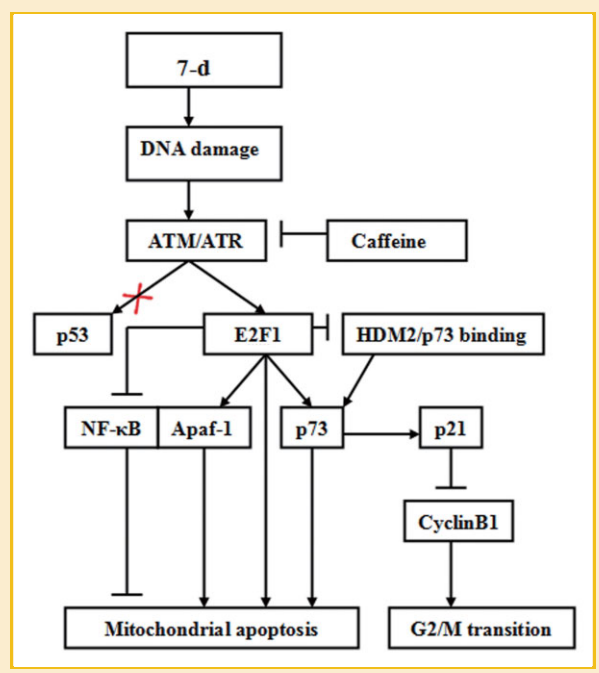

Fig. 8. Proposed model for the mechanism of 7-d-induced DNA damage-mediated G2/M arrest and apoptosis in p53-deficient K562 cells. [Color figure can be seen in the online version of this article, available at http://wileyonlinelibrary.com/journal/jcb]

We consider this finding is specially valuable, because so many cancers are p53-deficient, the proposed working models for the molecular basis would provide insights for approaches to the development of effective chemotherapy by targeting appropriate signal transduction [Engelmann et al., 2010]. Meanwhile, as such, 7-d has the potential to be developed as a potent anticancer drug candidate against p53-deficient tumors, including most leukemia cell lines.

REFERENCES

Blagosklonny MV. 2002. P53: An ubiquitous target of anticancer drugs. Int J Cancer 98:161–166.

Blattner C, Sparks A, Lane D. 1999. Transcription factor E2F-1 is upregulated in response to DNA damage in a manner analogous to that of p53. Mol Cell Biol 19:3704–3713.

Carcagno AL, Ogara MF, Sonzogni SV, Marazita MC, Sirkin PF, Ceruti JM, Canepa ET. 2009. E2F1 transcription is induced by genotoxic stress through ATM/ATR activation. IUBMB Life 61:537–543.

Chen Z, Liang X, Zhang H, Xie H, Liu J, Xu Y, Zhu W, Wang Y, Wang X, Tan S, Kuang D, Qian X. 2010. A new class of naphthalimide-based antitumor agents that inhibit Topoisomerase II and induce lysosomal membrane permeabilization and apoptosis. J Med Chem 53:2589–2600.

Chiu S-J, Lee Y-J, Hsu T-S, Chen W-S. 2009. Oxaliplatin-induced gamma-H2AX activation via both p53-dependent and -independent pathways but is not associated with cell cycle arrest in human colorectal cancer cells. Chemico Biol Inter 182:173–182.

Di Cintio A, Di Gennaro E, Budillon A. 2010. Restoring p53 function in cancer: Novel therapeutic approaches for applying the brakes to tumorigenesis. Recent Pat Anticancer Drug Discov 5:1–13.

Engelmann D, Knoll S, Ewerth D, Steder M, Stoll A, Puetzer BM. 2010. Functional interplay between E2F1 and chemotherapeutic drugs defines immediate E2F1 target genes crucial for cancer cell death. Cell Mol Life Sci 67:931–948.

Feinstein E, Cimino G, Gale RP, Alimena G, Berthier R, Kishi K, Goldman J, Zaccaria A, Berrebi A, Canaani E. 1991. p53 in chronic myelogenous leukemia in acute phase. Proc Natl Acad Sci USA 88:6293–6297.

Fueyo J, Gomez-Manzano C, Yung WK, Liu TJ, Alemany R, McDonnell TJ, Shi X, Rao JS, Levin VA, Kyritsis AP. 1998. Overexpression of E2F-1 in glioma triggers apoptosis and suppresses tumor growth in vitro and in vivo. Nat Med 4:685–690.

Furukawa Y, Furukawa Y, Nishimura N, Satoh M, Endo H, Iwase S, Yamada H, Matsuda M, Kano Y, Nakamura M. 2002. Apaf-1 is a mediator of E2F-1-induced apoptosis. J Biol Chem 277:39760–39768.

Gao WY, Tian ZY, Xie SQ, Mei ZH, Zhao J, Wang CJ. 2009. Conjugation of substituted naphthalimides to polyamines as cytotoxic agents targeting the Akt/mTOR signal pathway. Org Biomol Chem 7:4651–4660.

Ghobrial IM, Witzig TE, Adjei AA. 2005. Targeting apoptosis pathways in cancer therapy. CA Cancer J Clin 55:178–194.

Ginsberg D. 2002. E2F1 pathways to apoptosis. FEBS Lett 529:122–125.

Ginsberg D, Polager S. 2009. p53 and E2f: Partners in life and death. Nat Rev Cancer 9:738–748.

Goldschneider D, Blanc E, Raguenez G, Barrois M, Legrand A, Le Roux G, Haddada H, Benard J, Douc-Rasy S. 2004. Differential response of p53 target genes to p73 overexpression in SH-SY5Y neuroblastoma cell line. J Cell Sci 117:293–301.

Gorgoulis VG, Tsantoulis PK. 2005. Involvement of E2F transcription factor family in cancer. Eur J Cancer 41:2403–2414.

Hershko T, Ginsberg D. 2004. Up-regulation of Bcl-2 homology 3 (BH3)-only proteins by E2F1 mediates apoptosis. J Biol Chem 279:8627–8634.

Huang S, Norton JT, Witsch MA, Luong L, Kawamura A, Ghosh S, Stack MS, Sim E, Avram MJ, Appella DH. 2008. Synthesis and anticancer activities of 6-amino amonafide derivatives. Anti Cancer Drugs 19:23–36.

Ingrassia L, Lefranc F, Kiss R, Mijatovic T. 2009. Naphthalimides and azonafides as promising anti-cancer agents. Curr Med Chem 16:1192–1213.

Karbasian Esfahani M, Morris EL, Dutcher JP, Wiernik PH. 2006. Blastic phase of chronic myelogenous leukemia. Curr Treat Options Oncol 7:189–199.

Kitagawa R, Kastan MB. 2005. The ATM-dependent DNA damage signaling pathway. Cold Spring Harb Symp Quant Biol 70:99–109.

Ko SG, Kim HP, Jin DH, Bae HS, Kim SH, Park CH, Lee JW. 2005. Saussurea lappa induces G2-growth arrest and apoptosis in AGS gastric cancer cells. Cancer Lett 220:11–19.

Kojima K, Konopleva M, Samudio IJ, Shikami M, Cabreira-Hansen M, McQueen T, Ruvolo V, Tsao T, Zeng Z, Vassilev LT, Andreeff M. 2005. MDM2 antagonists induce p53-dependent apoptosis in AML: Implications for leukemia therapy. Blood 106:3150–3159.

Kuo LJ, Yang LX. 2008. Gamma-H2AX - a novel biomarker for DNA double-strand breaks. In Vivo 22:305–309.

Kurz EU, Lees-Miller SP. 2004. DNA damage-induced activation of ATM and ATM-dependent signaling pathways. DNA Repair (Amst) 3:889–900.

Kwon TK, Lee TJ, Kim OH, Kim YH, Lim JH, Kim S, Park JW. 2006. Quercetin arrests G2M phase and induces caspase-dependent cell death in U937 cells. Cancer Lett 240:234–242.

La Thangue NB, Stevens C. 2004. The emerging role of E2F-1 in the DNA damage response and checkpoint control. DNA Repair 3:1071–1079.

Lau LM, Nugent JK, Zhao X, Irwin MS. 2008. HDM2 antagonist Nutlin-3 disrupts p73-HDM2 binding and enhances p73 function. Oncogene 27:997–1003.

Law JC, Ritke MK, Yalowich JC, Leder GH, Ferrell RE. 1993. Mutational inactivation of the p53 gene in the human erythroid leukemic K562 cell line. Leuk Res 17:1045–1050.

Levites Y, Youdim MBH, Maor G, Mandel S. 2002. Attenuation of 6-hydroxydopamine (6-OHDA)-induced nuclear factor-kappaB (NF-kappa B) activation and cell death by tea extracts in neuronal cultures. Biochem Pharmacol 63:21–29.

Liang X, Wu A, Xu Y, Xu K, Liu J, Qian X. 2011. B1, a novel naphthalimide-based DNA intercalator, induces cell cycle arrest and apoptosis in HeLa cells via p53 activation. Invest New Drugs 29:646–658.

Liang X, Xu Y, Xu K, Liu J, Qian X. 2010. B1, a novel amonafide analogue, overcomes the resistance conferred by Bcl-2 in human promyelocytic leukemia HL60 cells. Mol Cancer Res 8:1619–1632.

Lin Y, Bai L, Chen W, Xu S. 2010. The NF-kappaB activation pathways, emerging molecular targets for cancer prevention and therapy. Expert Opin Ther Targets 14:45–55.

Liontos M, Niforou K, Velimezi G, Vougas K, Evangelou K, Apostolopoulou K, Vrtel R, Damalas A, Kontovazenitis P, Kotsinas A, Zoumpourlis V, Tsangaris GT, Kittas C, Ginsberg D, Halazonetis TD, Bartek J, Gorgoulis VG. 2009. Modulation of the E2F1-driven cancer cell fate by the DNA damage response machinery and potential novel E2F1 targets in osteosarcomas. Am J Pathol 175:376–391.

Liu JW, Yang F, Zhang Y, Li JY. 2007. Studies on the cell-immunosuppressive mechanism of Oridonin from Isodon serra. Int Immunopharmacol 7:945–954.

Lu H, Zeng XY, Chen LH, Jost CA, Maya R, Keller D, Wang XJ, Kaelin WG, Oren M, Chen JD. 1999. MDM2 suppresses p73 function without promoting p73 degradation. Mol Cell Biol 19:3257–3266.

Lv M, Xu H. 2009. Overview of naphthalimide analogs as anticancer agents. Curr Med Chem 16:4797–4813.

Olive PL, Banath JP. 2006. The comet assay: A method to measure DNA damage in individual cells. Nat Prot 1:23–29.

Pomerantz J, Schreiber-Agus N, Liegeois NJ, Silverman A, Alland L, Chin L, Potes J, Chen K, Orlow I, Lee HW, Cordon-Cardo C, DePinho RA. 1998. The

Ink4a tumor suppressor gene product, p19Arf, interacts with MDM2 and neutralizes MDM2's inhibition of p53. Cell 92:713–723.

Raghuvar Gopal DV, Narkar AA, Badrinath Y, Mishra KP, Joshi DS. 2005. Betulinic acid induces apoptosis in human chronic myelogenous leukemia (CML) cell line K-562 without altering the levels of Bcr-Abl. Toxicol Lett 155:343–351.

Rawat DS. 2008. Hot topic: Recent advances in cancer chemotherapy - Part I. Anti Cancer Agents Med Chem 8:122–122.

Sarkaria JN, Busby EC, Tibbetts RS, Roos P, Taya Y, Karnitz LM, Abraham RT. 1999. Inhibition of ATM and ATR kinase activities by the radiosensitizing agent, caffeine. Cancer Res 59:4375–4382.

Schlott T, Quentin T, Korabiowska M, Budd B, Kunze E. 2004. Alteration of the MDM2-p73-P14ARF pathway related to tumour progression during urinary bladder carcinogenesis. Int J Mol Med 14:825–836.

Stanelle J, Putzer BM. 2006. E2F1-induced apoptosis: Turning killers into therapeutics. Trends Mol Med 12:177–185.

Verma M, Singh SK, Bhushan S, Sharma VK, Datt P, Kapahi BK, Saxena AK. 2008. In vitro cytotoxic potential of Polyalthia longifolia on human cancer cell lines and induction of apoptosis through mitochondrial-dependent pathway in HL-60 cells. Chem Biol Interact 171:45–56.

Wallace HM, Palmer AJ. 2010. The polyamine transport system as a target for anticancer drug development. Amino Acids 38:415–422.

Wang G, Chen H, Huang M, Wang N, Zhang J, Zhang Y, Bai G, Fong WF, Yang M, Yao X. 2006. Methyl protodioscin induces G2/M cell cycle arrest and apoptosis in HepG2 liver cancer cells. Cancer Lett 241:102–109.

Weller M. 1998. Predicting response to cancer chemotherapy: The role of p53. Cell Tissue Res 292:435–445.

Wu Z, Yu Q. 2009. E2F1-mediated apoptosis as a target of cancer therapy. Curr Mol Pharmacol 2:149–160.

Wu Z, Zheng S, Yu Q. 2009. The E2F family and the role of E2F1 in apoptosis. Int J Biochem Cell Biol 41:2389–2397.